

# Thermodynamic Considerations of "Solid State Engines" Based on Thermoelastic Martensitic Transformations and the Shape Memory Effect

H. C. TONG AND C. M. WAYMAN

Engine applications of the shape memory ("Marmem") effect associated with thermoelastic transformations are discussed. Such devices potentially enable the direct conversion of heat (*i.e.*, solar energy or waste heat) into mechanical work. It is shown that efficiencies on the order of 20 pct may be expected and can be improved with alloys having certain transformation hysteresis loop characteristics.

It is well known from the law of degradation that energy can be taken from nature and put into useful forms. Electrical energy, for example, can be generated by changes in water level, nuclear reactions, and so on. Mechanical energy can be generated from phase transitions (physical or chemical) through converters such as steam or internal combustion engines. More recently, it has become apparent that alloys showing the well-known shape memory ("marmem")<sup>1</sup> effect generate substantial stresses upon heating, thus converting heat directly into mechanical work. Indeed a variety of "engine" applications are envisioned.<sup>1</sup> While no attempt at chronology is intended here, it can be noted that as early as 1957, the late Professor T. A. Read and colleagues at the University of Illinois constructed a cyclic weight lifting device (operating between two temperatures and employing a Au-47.5 pct Cd alloy) for exhibition at the 1958 World's Fair in Brussels. Within the past year, an engineering-wise more sophisticated version of such an engine apparatus has also been described by workers at the University of California.<sup>2</sup>

Notwithstanding previous efforts, it remains that detailed and quantitative analysis of the engine characteristics of shape memory materials in both fundamental thermodynamic and metallurgical terms has not been presented. This is the purpose of the present paper. After discussing pertinent background literature on thermoelastic martensitic transformations,<sup>1,3-5</sup> the magnitude of the mechanical energy gain from this type of solid state transformation will be discussed and the efficiency of the conversion process is analyzed. In addition to the analysis of a solid state engine, the efficiency of a Carnot engine working within the same temperature limits is used for comparison.

## THERMOELASTIC BEHAVIOR AND THE SHAPE MEMORY EFFECT

Well after the familiar martensitic transformation in steels become commonly known<sup>6</sup> Kurdjumov and co-

workers<sup>7</sup> in 1938 observed a *reversible* martensitic transformation upon cooling and heating certain Cu-Zn and Cu-Al alloys. It was also suggested<sup>5</sup> that a "thermoelastic" equilibrium exists for such reversible alloys which is characterized by the fact that these alloys can transform into martensite either by decreasing the temperature or by applying a stress at temperatures above the  $M_s$  temperature. Correspondingly, the reverse transformation could be induced by either raising the temperature or by removing an applied stress.

In 1951, Chang and Read<sup>3</sup> observed that Au-Cd alloys also showed thermoelastic behavior. In addition, they found that a Au-47.5 at. pct Cd alloy was very soft in the martensitic state and could be deformed rather easily, the deformed shape being recovered during the reverse transformation to the parent phase. There was no permanent set remaining after the shape was recovered during the reverse transformation process. This behavior is now known to typify the shape memory effect.

Since the work of Chang and Read, a number of alloys exhibiting the shape memory behavior have been reported, among which are the systems Ti-Ni,<sup>4</sup> In-Tl,<sup>8</sup> Cu-Al-Ni,<sup>7</sup> Cu-Zn,<sup>10</sup> Fe-Pt,<sup>10</sup> and Ag-Cd.<sup>11</sup> All of these alloys exhibit a thermoelastic martensitic transformation, and with the exception of the In-Tl system, all involve a martensitic transformation from an ordered parent phase. Further, these materials exhibit a rather small transformation hysteresis loop, as determined by electrical resistance measurements, for example. A general review of shape memory ("Marmem") alloys has been presented by Wayman and Shimizu.<sup>1</sup> Recently, it has been verified<sup>11,12</sup> that alloys deformed below the  $M_f$  temperature begin the shape recovery process at the  $A_s$  temperature on heating; the deformed shape is completely recovered at the  $A_f$  temperature. The stress dependence of the  $M_s$ ,  $M_f$ ,  $A_s$ , and  $A_f$  temperatures has also been discussed recently.<sup>13</sup>

Lattice softening prior to thermoelastic martensitic transformations appears to be another common characteristic.<sup>14</sup> The shear constant  $(C_{11} - C_{12})/2$  decreases when an alloy approaches the  $M_s$  temperature. As a consequence, transformations can be induced by a small shear stress component exerted near  $M_s$ . Certain alloys are also physically soft below the  $M_f$  temperature, in which case a small stress results in a

H. C. TONG, formerly with the University of Illinois is now with General Product Division, IBM Corporation, San Jose, California. C. M. WAYMAN is Professor of Metallurgy at the University of Illinois at Urbana-Champaign, Urbana, Illinois.

Manuscript submitted May 23, 1974.

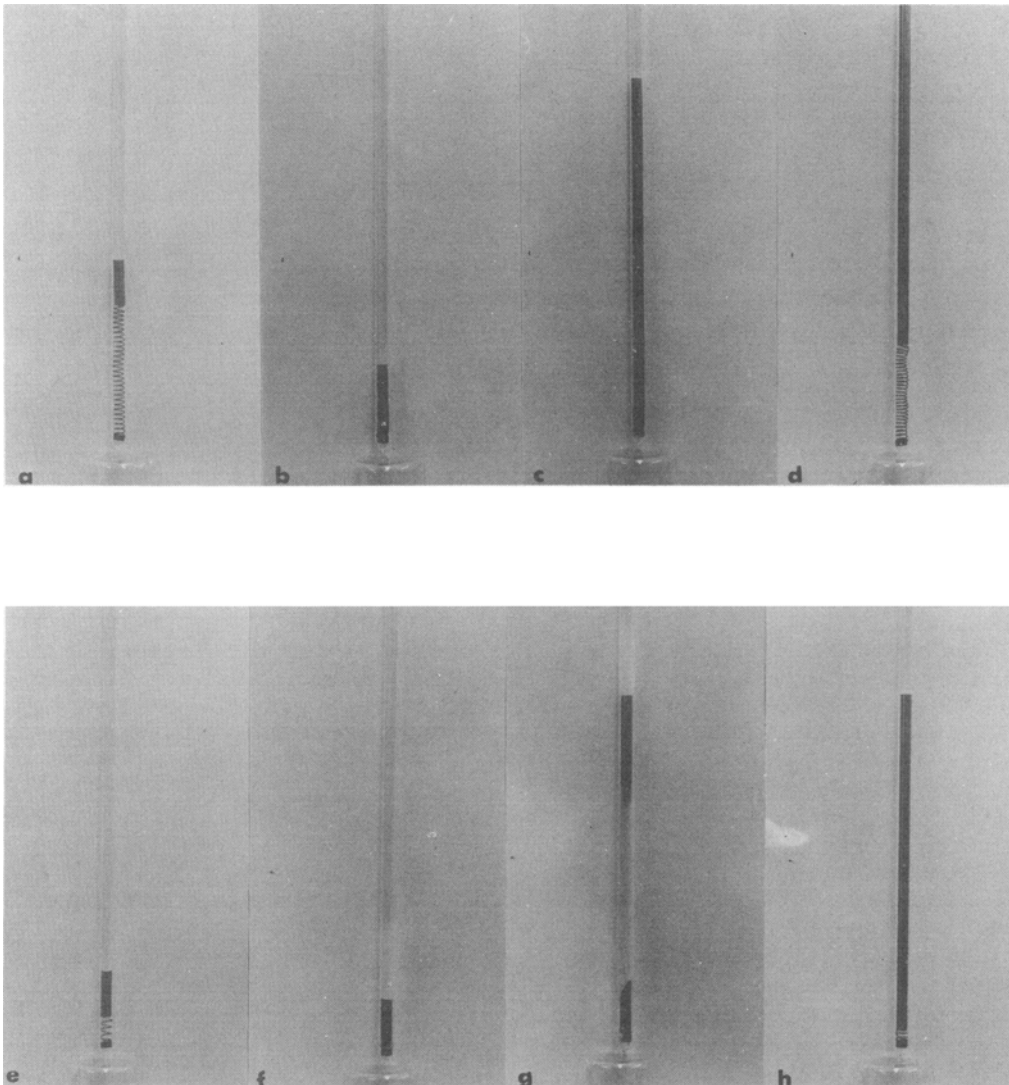


Fig. 1—Demonstration of model thermal  $\rightarrow$  mechanical energy conversion apparatus (Small plunger  $\sim$  20 g; larger plunger  $\sim$  180 g). Upper, NiTi Coil: (a) 20°C, (b) 0°C, (c) 0°C, (d) 70°C. Lower, AgCd Coil: (e) 20°C, (f)  $\sim$  100°C, (g)  $\sim$  100°C, (h) 20°C.

substantial pseudoplastic\* strain<sup>15</sup> which is entirely

\*The term pseudo-plastic is used because the apparent plastic deformation below  $M_f$  is recovered during the reverse transformation.

recovered on heating.

The shape recovery process begins at  $A_s(\sigma)$  and is completed when  $A_f(\sigma)$  is reached. This notation is followed since the  $A_s$ ,  $A_f$ ,  $M_s$ , and  $M_f$  temperatures are stress-dependent. The higher the applied stress,  $\sigma$ , exerted in the martensitic state, the higher will be the  $A_s(\sigma)$  and  $A_f(\sigma)$  temperatures. Thus, a load applied on a specimen in the martensitic condition will result in a back stress in opposition to the load when the specimen is heated to regain its original shape. Work is therefore performed against the load. The minimum stress,  $\sigma_1$ , to pseudoplastically deform the specimen in the martensitic state is much smaller than the maximum stress  $\sigma_m$ , which if exceeded would not permit perfect shape recovery during heating through the reverse transformation (under stress). The present work indicates that  $\sigma_m$  can be as large as ten times  $\sigma_1$ . If the pseudoplastic martensite deformation and subsequent shape recovery on heating under stress involve a comparatively large displacement,  $\Delta l$ , relative to the original specimen length, the net work done,

$\int_0^{\Delta l} (\sigma_m - \sigma_1) dl$ , becomes significant, and the thermal energy can be transformed into mechanical energy. This characteristic suggests that a solid state engine is feasible.

#### AN EXAMPLE

Two different alloys were used to demonstrate the above-mentioned feasibility: Ti-55.6 wt pct Ni and Ag-46 at. pct Cd. Specimens were prepared in the form of springs while in the parent phase condition. At temperatures above the  $A_s(\sigma)$  temperature (*i.e.*, room temperature), both specimens could support the weight of a 20 g steel plunger, as shown in Figs. 1(a) and 1(e). When the specimens were cooled to their  $M_f$  temperatures, both coils collapsed pseudoplastically under the weight of the 20 g plunger, Figs. 1(b) and 1(f). After the pseudoplastic deformation at  $M_f$ , a 180 g steel rod was used to replace the 20 g rod, Figs. 1(c) and 1(g). In both cases, when the coils were heated to a temperature (room temperature for Ag-Cd; 70°C for Ti-Ni) above  $A_f(\sigma)$  they were observed to lift the 180 g weight, and only elastic deformation of the parent phase remained (Figs. 1(d) and 1(h)).

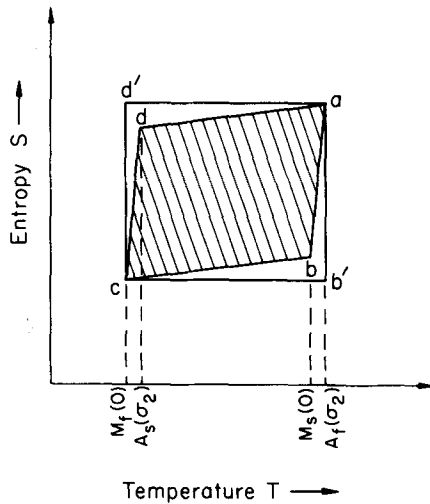


Fig. 2—Schematic Temperature ( $T$ ) vs. Entropy ( $S$ ) diagram for thermal to mechanical energy conversion cycle. (See text for discussion).

### EFFICIENCY

As noted above, thermal energy can be converted into mechanical energy by means of the shape memory effect. The work done/cycle and the efficiency of the conversion process can be analyzed. Accordingly, we consider a rod-shaped cylindrical specimen of unit mass, length  $l_0$  and cross section  $A_0$ . In general, the  $M_s$ ,  $M_f$ ,  $A_s$ , and  $A_f$  temperatures in thermoelastic martensitic transformations are stress-dependent and will be designated  $M_s(\sigma)$ ,  $M_f(\sigma)$ ,  $A_s(\sigma)$ , and  $A_f(\sigma)$ , and for the zero stress case are denoted  $M_s(0)$ ,  $M_f(0)$ ,  $A_s(0)$ , and  $A_f(0)$ . The  $M_s$  and  $M_f$  temperatures correspond to the start and finish temperatures for the parent to martensite ( $P \rightarrow M$ ) transformation while  $A_s$  and  $A_f$  are the start and finish temperatures for the reverse martensite to parent ( $M \rightarrow P$ ) transformation.

For purposes of analysis, the temperature-entropy diagram shown in Fig. 2 is used. The specimen is first cooled from  $T_a$  to  $M_f(0)$  under no stress. A stress  $\sigma_1$  is then applied which strains the specimen pseudo-plastically to a value  $\epsilon = \Delta l/l_0$ . The stress  $\sigma_1$  is small in relation to  $\sigma_m$ , the stress above which perfect strain recovery upon heating through the reverse transformation would not occur. Next a stress  $\sigma_2$  ( $\sigma_m > \sigma_2 \gg \sigma_1$ ) is applied at  $M_f(0)^*$  and the specimen is heated until com-

\*Since  $\sigma_1 \ll \sigma_2$ , it is a reasonable approximation in the temperature-entropy cycle to take  $M_f(\sigma_1) = M_f(0)$ .

plete reversal of the martensite occurs. This is accomplished at  $T_a = A_f(\sigma_2)$ . Note that because of the relative magnitude of  $\sigma_2$ , the  $A_s$  and  $A_f$  temperatures under stress ( $\sigma_2$ ) are displaced to higher levels. During the reverse transformation, work is done against the stress  $\sigma_2$ , the magnitude of the load is  $\sigma_2 A_0$ . The second cycle is then started at  $T_a$  under zero stress. Since, by definition, the specimen exists in the parent phase at  $A_f(\sigma_2)$ , no change (*i.e.*, transformation) occurs when  $\sigma_2$  is removed before the no-stress portion of the transformation cycle is started. If the volume change due to the phase transformation is small,\* the

\*In known thermoelastic martensitic transformations the volume change is less than one percent.

work done by the specimen is

$$W = - \int_{l_0}^l A \sigma_2 dl = \sigma_2 V_0 \ln(1 + \epsilon) \quad [1]$$

where  $\epsilon = (l - l_0)/l_0$  and  $V_0 = A_0 l_0$ . The net work done by the specimen is then

$$W_{\text{net}} = (\sigma_2 - \sigma_1) V_0 \ln(1 + \epsilon) \quad [2]$$

The equilibrium temperature  $T_0(0)$  at the zero stress level can be shifted by an externally applied stress. This relationship has previously been shown<sup>13</sup> to be

$$T_0(\sigma) = T_0(0) + C\sigma \quad [3]$$

where  $C$  is a constant. Eq. [3] can be directly related to the Clausius-Clapeyron equation<sup>14</sup> following which

$$C = \frac{T_0(0) V_0 \epsilon}{\Delta Q}$$

and

$$\Delta T_0 = T_0(\sigma) - T_0(0) = \frac{T_0(0) V_0 \epsilon \sigma}{\Delta Q} \quad [4]$$

where  $\Delta Q$  is the transformation latent heat. Eq. [2] can be further simplified to

$$\begin{aligned} W_{\text{net}} &\approx \sigma_2 V_0 \ln(1 + \epsilon) \text{ if } \sigma_1 \ll \sigma_2 \\ &= \sigma_2 \epsilon V_0 \frac{\ln(1 + \epsilon)}{\epsilon} \\ &= \Delta Q \left( \frac{\Delta T_0}{T_0(0)} \right) \left( \frac{\ln(1 + \epsilon)}{\epsilon} \right) \end{aligned} \quad [5]$$

Since the work done on the specimen by the stress  $\sigma_1$  is negligible in relation to the work done by it against the stress  $\sigma_2$ , the work input will be neglected. The appropriate thermal cycle as shown by the temperature-entropy diagram of Fig. 2 consists of a:  $A_f(\sigma_2) \rightarrow b$ :  $M_s(0) \rightarrow c$ :  $M_f(0) \rightarrow d$ :  $A_s(\sigma_2) \rightarrow a$ :  $A_f(\sigma_2)$ . For the same temperature limits the Carnot engine cycle is a:  $A_f(\sigma_2) \rightarrow b' \rightarrow c$ :  $M_f(0) \rightarrow d' \rightarrow a$ :  $A_f(\sigma_2)$ . Process  $a \rightarrow b$  indicates that the parent phase is being cooled from  $A_f(\sigma_2)$  to  $M_s(0)$ ; process  $b \rightarrow c$  corresponds to the formation of martensite between  $M_s(0)$  and  $M_f(0)$ , during which the latent heat  $\Delta Q$  is released; process  $c \rightarrow d$  indicates heating the martensitic phase from  $M_f(0)$  to  $A_s(\sigma_2)$ ; and the final step  $d \rightarrow a$  represents the reverse martensite transformation from  $A_s(\sigma_2)$  to  $A_f(\sigma_2)$  during which the latent heat  $\Delta Q$  is absorbed.

From the thermal cycle described above the heat absorbed during processes  $c \rightarrow d$  and  $d \rightarrow a$  is respectively

$$\begin{aligned} \int_{M_f(0)}^{A_s(\sigma_2)} C_P^M dT \quad \text{and} \\ \int_{A_s(\sigma_2)}^{A_f(\sigma_2)} [f_P^{M \rightarrow P} C_P^P + (1 - f_P^{M \rightarrow P}) C_P^M] dT + \Delta Q \end{aligned} \quad [6]$$

where  $C_P^P$  and  $C_P^M$  are the specific heats of the parent and martensitic phases and  $f_P^{M \rightarrow P}$  is the volume fraction of the parent phase present during the reverse transformation, which is temperature dependent. The efficiency for the thermal cycle is then

$$\eta = \frac{\Delta Q \left( \frac{\Delta T_0}{T_0(0)} \right) \left( \frac{\ln(1 + \epsilon)}{\epsilon} \right)}{\Delta Q + \int_{M_f(0)}^{A_s(\sigma_2)} C_P^M dT + \int_{A_s(\sigma_2)}^{A_f(\sigma_2)} [f_P^{M \rightarrow P} C_P + (1 - f_P^{M \rightarrow P}) C_P^M] dT} \quad [7]$$

For simplicity the mean  $C_P$  values  $\bar{C}_P^M$  and  $\bar{C}_P^P$  are taken over the temperature range  $M_f(0)$  to  $A_f(\sigma_2)$ , and it is further assumed that  $f_P^{M \rightarrow P}$  is proportional to the

temperature difference  $[T - A_s(\sigma_2)]$ . Eq. [7] then becomes

$$\eta = \frac{\Delta Q \left( \frac{\Delta T_0}{T_0(0)} \right) \left( \frac{\ln(1 + \epsilon)}{\epsilon} \right)}{\Delta Q + \bar{C}_P^M (A_s(\sigma_2) - M_f(0)) + 1/2 \{ \bar{C}_P^P [A_f(\sigma_2) - A_s(\sigma_2)] + \bar{C}_P^M [A_f(\sigma_2) - A_s(\sigma_2)] \}} \quad [8]$$

## DISCUSSION AND CONCLUSIONS

From Fig. 2, a Carnot cycle working under the same temperature limits as the model engine has an efficiency

$$\eta_c = 1 - \frac{M_f(0)}{A_f(\sigma_2)} \quad [9]$$

and as obvious from the  $T$ - $S$  diagram, the Carnot cycle is the more efficient of the two. Since  $A_f(\sigma_2)$  can be written as

$$\begin{aligned} A_f(\sigma_2) &= A_f(0) + A_f(\sigma_2) - A_f(0) \\ &= A_f(0) + \left( \frac{\Delta T_0}{T_0(0)} \right) T_0(0) \end{aligned} \quad [10]$$

(using the approximation  $[A_f(\sigma_2) - A_f(0)] \approx [T_0(\sigma_2) - T_0(0)] = \Delta T_0$  the Carnot cycle efficiency can be rewritten as

$$\eta_c = 1 - \frac{M_f(0)}{A_f(0) + \left( \frac{\Delta T_0}{T_0(0)} \right) T_0(0)} \quad [11]$$

Considering the same stresses as before, the present thermal cycle can be simplified by taking

$$\Delta T_0 \gg [A_s(0) - M_f(0)]^*$$

$$\Delta T_0 \gg [A_f(0) - A_s(0)]^*$$

$$\bar{C}_P \approx \bar{C}_P^P \approx \bar{C}_P^M$$

\*For example, using experimental data (electrical resistivity vs. temperature plots) from a Ag<sub>47.8</sub>at pct Cd alloy,  $[A_s(0) - M_f(0)] \approx 7\text{K}$ ,  $[A_f(0) - A_s(0)] \approx 10\text{K}$  and  $\Delta T_0(\text{max}) \approx 80\text{K}$ .<sup>11</sup>

and by assuming that supercooling and superheating are independent of stress. Eq. [8] can thus be simplified to

$$\begin{aligned} \eta &= \frac{\Delta Q \left( \frac{\Delta T_0}{T_0(0)} \right) \left( \frac{\ln(1 + \epsilon)}{\epsilon} \right)}{\Delta Q + \bar{C}_P \Delta T_0} \\ &= \left( \frac{\ln(1 + \epsilon)}{\epsilon} \right) \left( \frac{1}{T_0(0)} \right) \left( \frac{1}{1/\Delta T_0 + \bar{C}_P/\Delta Q} \right) \end{aligned} \quad [12]$$

Letting  $\epsilon = 0.10$ ,  $\bar{C}_P = 4$  cal/mole K (18.55 J/kg K),  $\Delta Q = 100$  cal/mole (464 J/kg),  $T_0 = 100$  K,  $\Delta T_0 = 100$  K,  $A_f = 110$  K, and  $M_f = 70$  K. Eqs. [11] and [12] respectively give  $\eta_c = 0.67$  and  $\eta = 0.20$ , which shows again that  $\eta_c > \eta$ . It should be emphasized that Eq. [12] is only a rough approximation.

The previous analysis and approximate efficiency of 20 pct indicate that it may be feasible to apply the thermal to mechanical conversion properties of thermoelastic martensitic materials to convert solar energy and other wasted heat into mechanical energy. Thus the notion of a solid state engine working on solar energy is suggested for future development. It follows that optimum selection of materials may lead to higher efficiencies. Although Eq. [12] is only an approxima-

tion, it nevertheless serves as a guide for selecting materials with desirable characteristics. The following items are thus considered essential for the energy converter.

1. The material must exhibit a thermoelastic martensitic transformation so that the shape memory behavior is preserved over many cycles.
2. Following the previous, a long fatigue life under reasonably high stress levels is required.
3. The parent phase yield stress should be as high as possible in order to maximize  $\Delta T_0$ .
4.  $T_0(0)$  should be reasonably low.
5. The recoverable strain,  $\epsilon$ , should be large.
6. A large latent heat,  $\Delta Q$ , favors a higher efficiency.

In general, recoverable strains on the order of 8 to 10 pct have been determined for Cu-Zn,<sup>16</sup> Ag-Cd,<sup>17</sup> and Ti-Ni<sup>18</sup> alloys, and in the latter case an exceptionally high fatigue life is found.<sup>18</sup> It is also known that  $T_0(0)$  can be regulated by alloying. However, many of the above features remain to be studied in detail. Although thermoelastic martensitic transformations have been appreciated for some time, it is only recently that they have attracted attention, particularly because of the shape memory effect and certain indicated applications. It is emphasized here that thermal-mechanical energy conversion is only one of many likely future applications. The need is already clear for systematic alloy development, property measurements, and innovations of devices.

This work was partially supported by the Atomic Energy Commission and the National Science Foundation.

## REFERENCES

1. C. M. Wayman and K. Shimizu: *Metal Sci. J.*, 1972, vol. 6, p. 175.
2. P. Hernandez, Lawrence Radiation Laboratory, University of California at Berkeley, private communication, 1974.
3. L. C. Chang and T. A. Read: *Trans. AIME*, 1951, vol. 189, p. 47.
4. F. E. Wang, W. J. Buehler, and S. J. Pickart, *J. Appl. Phys.*, 1965, vol. 36, p. 3232.
5. G. V. Kurdjumov and L. G. Khandros: *Doklady Akad. Nauk S. S. R.*, 1949, vol. 66, p. 221.
6. F. Osmond: Bulletin, Society de Encouragement pour l'Industrie Nationale, vol. 10, p. 480 (1895).
7. G. Kurdjumov, I. Isaitschew, and E. Kaminsky: *Trans. AIME*, 1938, vol. 128, p. 361.
8. Z. S. Basinski and J. W. Christian: *Acta Met.*, 1954, vol. 2, p. 161.
9. K. Otsuka and K. Shimizu, *Scripta Met.*, 1970, vol. 4, p. 469.
10. C. M. Wayman: *Scripta Met.*, 1971, vol. 5, p. 489.
11. H. C. Tong and C. M. Wayman: *Scripta Met.*, 1973, vol. 7, p. 215.
12. K. Otsuka, K. Shimizu, I. Cornelis, and C. M. Wayman: *Scripta Met.*, 1972, vol. 5, p. 377.
13. H. C. Tong and C. M. Wayman: *Scripta Met.*, 1974, vol. 8, p. 93.
14. N. Nakanishi, T. Mori, S. Miura, Y. Murakami, and S. Kachi: *Phil. Mag.*, 1973, vol. 28, p. 277.
15. R. V. Krishnan and L. C. Brown: *Met. Trans.*, 1973, vol. 4, p. 423.
16. T. A. Schroeder, M. S. Thesis, University of Illinois, May 1974.
17. H. C. Tong and C. M. Wayman, unpublished work.
18. W. J. Buehler and F. E. Wang: *Ocean Eng.*, 1968, vol. 1, p. 105.